Technical Paper
J. Astron. Space Sci. 32(3), 257-268 (2015)
http://dx.doi.org/10.5140/JASS.2015.32.3.257

JASS Journal of Astronomy and Space Sciences

Preliminary Analysis of Delta-V Requirements for a Lunar CubeSat Impactor with Deployment Altitude Variations

Young-Joo Song[1†], Jin Ho[2], Bang-Yeop Kim[1]

[1]Lunar Exploration Mission Team, Korea Aerospace Research Institute, Daejeon 34133, Korea
[2]School of Space Research, Kyung Hee University, Yongin 17104, Korea

Characteristics of delta-V requirements for deploying an impactor from a mother-ship at different orbital altitudes are analyzed in order to prepare for a future lunar CubeSat impactor mission. A mother-ship is assumed to be orbiting the moon with a circular orbit at a 90 deg inclination and having 50, 100, 150, 200 km altitudes. Critical design parameters that are directly related to the success of the impactor mission are also analyzed including deploy directions, CubeSat flight time, impact velocity, and associated impact angles. Based on derived delta-V requirements, required thruster burn time and fuel mass are analyzed by adapting four different miniaturized commercial onboard thrusters currently developed for CubeSat applications. As a result, CubeSat impact trajectories as well as thruster burn characteristics deployed at different orbital altitudes are found to satisfy the mission objectives. It is concluded that thrust burn time should considered as the more critical design parameter than the required fuel mass when deducing the onboard propulsion system requirements. Results provided through this work will be helpful in further detailed system definition and design activities for future lunar missions with a CubeSat-based payload.

Keywords: lunar cubesat impactor, Delta-V, impact trajectory

1. INTRODUCTION

More than one hundred CubeSats have been placed in orbit since the first launch of a CubeSat in 2003 (Swartwout 2013). CubeSats have been proven to allow for extremely low-cost missions in near Earth orbits with greater launch accessibility. As a result, ideas for applying CubeSat technology to deep space exploration concepts have greatly increased (Klesh & Castillo-Rogez 2012). Recently, the NASA Innovative Advanced Concepts (NIAC) program selected interplanetary CubeSats for further investigation in order to enable a new class of missions beyond low Earth orbits (Blaney et al. 2012). The potential missions initially considered by NIAC are: Mineral Mapping of an Asteroid, Solar System Escape Technology Demonstration, Earth-Sun Sub-L1 Space Weather Monitor, Phobos Sample Return, Earth-Moon L2 Radio Quiet Observatory, and Out-of-Ecliptic Missions (Staehle et al. 2013). In addition to these missions, NASA is considering launching a CubeSat-based payload on a future Mars exploration mission around 2016 to early 2020's using excess capacity on the mission's primary spacecraft (Komarek et al. 2013). Recently, the Jet Propulsion Laboratory (JPL) selected and funded CubeSat concept studies for the NASA mission Europa Clipper, of which a mission is aimed for launch around 2025 with multiple CubeSats. Scientific objectives for the released CubeSats in the Jovian system would include determining reconnaissance for future landing sites, gravity fields, magnetic fields, atmospheric and plume conditions, and radiation levels in order to enhance our understanding of Europa (JPL 2013). Over the coming decade, it is expected that diverse scientific information could be obtained from

Received Jun 8, 2015 **Revised** Aug 7, 2015 **Accepted** Aug 7, 2015
†**Corresponding Author**
E-mail: dearyjs@kari.re.kr, ORCID: 0000-0001-6948-1920
Tel: +82-42-870-3915, Fax: +82-42-870-3919

extremely low-cost solar system exploration missions with improved CubeSat technologies that are beyond those that have been demonstrated to date (Staehle et al. 2013).

Since 1992, Korea has been continuously operating more than ten Earth-orbiting satellites and is now expanding its interests to planetary missions. The Korean space program has plans to launch a lunar orbiter and lander around 2020, and also has plans to explore Mars, asteroids, and deep space in the future. Therefore, the Korean aeronautical and space science community has performed numerous related mission studies, and the Korea Aerospace Research Institute (KARI) is performing pre-phase work for the lunar mission. Several preliminary design studies have already been conducted, such as an transfer trajectory analysis (Song et al. 2009, 2011; Woo et al. 2010), contact schedule analysis (Song et al. 2013, 2014), rover system design (Kim et al. 2009, Eom et al. 2012). For the lunar orbiter mission, the Korean lunar science committee is now working to select the main scientific objectives. One of the candidates is to fly a CubeSat impactor to explore lunar magnetic anomalies and associated albedo features, known as swirls (Lee et al. 2014). In 1959, the Soviet spacecraft called "Luna-1" carried a magnetometer to the Moon. Observation data from "Luna-1"concluded that the Moon has no global magnetic field like the Earth. However, from the Apollo 15 and 16 missions, it was discovered that strongly magnetized materials are distributed all over the Moon's crust. The origin of lunar magnetism is one of the oldest problems that is still being debated in the field of lunar science (Garrick-Bethell et al. 2013). Understanding the origin of swirls may help to understand not only geological processes, but also space weathering effects on the lunar surface. Although previous lunar missions such as NASA's Lunar Prospector and JAXA's KAGUYA also measured lunar magnetic fields, these data are not enough to completely characterize the magnetic anomaly region because they were obtained at high altitudes (>20 km) above the lunar surface (Garrick-Bethell et al. 2013). For this reason, a new idea proposes to use a CubeSat carrying a magnetometer as a payload to impact the target region of interest. The concept of using a CubeSat impactor to measure lunar magnetic fields near the surface has already been discussed by Garrick-Bethell et al. (2013). In the literature by Garrick-Bethell et al. (2013), two major lunar transfer scenarios are proposed to deliver the CubeSat impactor. The first option is to use the Planetary HitchHiker (PHH) concept, which involves a small spacecraft designed to be accommodated as a secondary payload on a variety of launch vehicles. In this concept, the launch vehicle places the PHH spacecraft into Geostationary Transfer Orbit (GTO) to reduce mission costs. Following insertion into GTO, the PHH spacecraft uses onboard propulsion to cruise to the Moon and, finally, releases the CubeSat impactor after appropriate orbital conditions are established. Appropriate orbital conditions to deploy the CubeSat impactor will be established by several Lunar Orbit Insertion (LOI), orbit adjustment, and station-keeping burns as is done during conventional lunar mission sequences. The second concept involves boarding the CubeSat impactor into a geostationary spacecraft as a payload and deploying it after reaching geostationary orbit (GEO). The released impactor will spiral out to the Moon with its own minimized ion propulsion system and upon entering the Moon's gravitational sphere of influence, the CubeSat will directly impact the target area without entering the lunar orbit. However, these two mission scenarios have several challenging aspects to overcome; longer flight times to reach the lunar orbit (which is expected to be more than 100 days), tolerating large amounts of radiation exposure even though the mission starts from GEO, and, most importantly, establishing a shallow impact angle (<10 deg) during the impact phase to meet the science objectives, which is a more critical factor if a mother-ship is not used (Garrick-Bethell et al. 2013).

Another promising method to achieve this mission objective might be to fly the lunar CubeSat impactor as one of the scientific payloads on the lunar orbiter. We believe that this approach will partly ease the challenging aspects that have been raised in the previously discussed scenarios, especially for establishing very shallow impact angles. Indeed, one of the major expected contributions of using CubeSats in planetary missions is that a large variety of near-surface scientific experiments could be performed (Klesh & Castillo-Rogez 2012). Most of planetary exploration to date has been performed through remote sensing from orbiters or by surface exploration using landers. However, such methods are expensive and risky and the scientific data gathered from near-surface can be limited (Klesh & Castillo-Rogez 2012). For these reasons, and as previously discussed, CubeSat-based payload planetary missions are vigorously promoted not only for the Moon, but also for Mars, Europa and other deep space exploration missions. Recently, Song et al. (2015) analyzed CubeSat impact trajectory characteristics as a function of its release conditions from a mother-ship orbiting the Moon at about a 100 km altitude. They also analyzed relative motions between the CubeSat and the mother-ship during the impact phase. From Song et al.'s (2015) work, it is found that a very shallow impact angle (less than 10 deg) could be achieved by releasing the CubeSat from a 100 km altitude. However, the amount of required divert delta-V magnitude to have the CubeSat to impact the lunar surface is found to be quite large

compared with the capabilities of the currently available Poly Picosatellite Orbital Deployer (P-POD) system. This means that a CubeSat on-board thruster is necessary to achieve the impact trajectory. Furthermore, required divert delta-V's with different CubeSat release altitudes should be further analyzed for diversities of mission analysis.

Therefore, impact trajectory characteristics and their dependence on release conditions from a mother-ship having different orbital altitudes are analyzed in the current work. Also, based on the derived delta-V requirements, required thruster burn time and fuel mass are analyzed by adapting four different miniaturized commercial onboard thrusters currently developed for CubeSat applications. The authors believe that these preliminary impact trajectory design studies will be helpful for further detailed system definition and design activities. In Section 2, system dynamics to establish the CubeSat impact problem is described in order to simulate a given impactor mission. Numerical assumptions made for the simulation are discussed in Section 3. Detailed analysis results are provided in Section 4 including impact trajectory characteristics as a function of deployment altitude and divert burn characteristics for different onboard thrusters. In Section 5, conclusions are made. Although the current analysis only considers a lunar CubeSat impactor mission, the methods discussed herein can easily be modified and applied to other similar missions where CubeSats are released from a mother-ship orbiting around another planet or moon, and will certainly have broad implications for future planetary missions involving CubeSats.

2. CUBESAT IMPACT PROBLEM

Two body equations of motion of the CubeSat impactor released from a mother-ship are expressed as:

$$\begin{bmatrix} \dot{\boldsymbol{r}} \\ \dot{\boldsymbol{v}} \end{bmatrix} = \begin{bmatrix} \boldsymbol{v} \\ -\dfrac{\mu \boldsymbol{r}}{r^3} \end{bmatrix} \tag{1}$$

with initial conditions

$$\begin{bmatrix} \boldsymbol{r}(0) \\ \boldsymbol{v}(0) \end{bmatrix} = \begin{bmatrix} \boldsymbol{r}_0 \\ \boldsymbol{v}_0 + \Delta \boldsymbol{v} \end{bmatrix} \tag{2}$$

where μ is the gravitational constant of the Moon, $\boldsymbol{r}$ and $\boldsymbol{v}$ denote position and velocity vectors, r is the magnitude of $\boldsymbol{r}$, $\boldsymbol{r}_0$ and $\boldsymbol{v}_0$ denote position and velocity vectors of a mother-ship at the time of the CubeSat's release, and $\Delta \boldsymbol{v}$ is the divert delta-V applied to release the CubeSat, respectively. Every vector in Eqs. (1) and (2) are expressed in the Moon-centered Moon Mean Equator and IAU vector of epoch J2000 (M-MME2000) frame. The divert delta-V applied to release the CubeSat can also be expressed in the mother-ship's Local Vertical/Local Horizontal (LVLH) frame, $\Delta \boldsymbol{v}^{LVLH}$, as follows (Vallado 2013)

$$\Delta \boldsymbol{v}^{LVLH} = \Delta v \cos(\alpha(t_r))\cos(\beta(t_r))\hat{\boldsymbol{i}} + \Delta v \sin(\alpha(t_r))\cos(\beta(t_r))\hat{\boldsymbol{j}} + \Delta v \sin(\beta(t_r))\hat{\boldsymbol{k}} \tag{3}$$

where $\Delta \boldsymbol{v}$ is the divert delta-V magnitude and $\alpha(t_r)$ and $\beta(t_r)$ are the defined in-plane and out-of-plane direction delta-V deploy angles, respectively, at the time of CubeSat release, which is denoted as t_r. In Eq. (3), $\hat{\boldsymbol{i}}$, $\hat{\boldsymbol{j}}$ and $\hat{\boldsymbol{k}}$ are the defined co-moving unit vectors in the transverse, opposite normal, and along the inward radial directions, respectively, all of which are attached to the mother-ship. The unit vectors are defined as follows: $\hat{\boldsymbol{k}}$ is the unit vector which always points from the mother-ship's center of the mass along the radius vector to the Moon's center; $\hat{\boldsymbol{j}}$ is the unit vector that lies in the opposite direction of the mother-ship's angular momentum vector, and $\hat{\boldsymbol{i}}$ is the unit transverse vector perpendicular to both $\hat{\boldsymbol{k}}$ and $\hat{\boldsymbol{j}}$ that points in the direction of the mother-ship's velocity vector. In addition, the defined $\alpha(t_r)$ is measured from the unit vector $\hat{\boldsymbol{i}}$ to the vector projected onto the local horizontal plane that is perpendicular to orbital plane. $\beta(t_r)$ is measured from the local horizontal plane to the delta-V vector in the vertical direction. $\Delta \boldsymbol{v}$ and $\Delta \boldsymbol{v}^{LVLH}$ can be transformed using the following relations: (Curtis 2009).

$$\Delta \boldsymbol{v} = \begin{bmatrix} \left(\dfrac{(-\boldsymbol{r}\times\boldsymbol{v})\times(-\boldsymbol{r})}{|(-\boldsymbol{r}\times\boldsymbol{v})\times(-\boldsymbol{r})|}\right)_x & \left(\dfrac{-\boldsymbol{r}\times\boldsymbol{v}}{|-\boldsymbol{r}\times\boldsymbol{v}|}\right)_x & \left(\dfrac{-\boldsymbol{r}}{|-\boldsymbol{r}|}\right)_x \\ \left(\dfrac{(-\boldsymbol{r}\times\boldsymbol{v})\times(-\boldsymbol{r})}{|(-\boldsymbol{r}\times\boldsymbol{v})\times(-\boldsymbol{r})|}\right)_y & \left(\dfrac{-\boldsymbol{r}\times\boldsymbol{v}}{|-\boldsymbol{r}\times\boldsymbol{v}|}\right)_y & \left(\dfrac{-\boldsymbol{r}}{|-\boldsymbol{r}|}\right)_y \\ \left(\dfrac{(-\boldsymbol{r}\times\boldsymbol{v})\times(-\boldsymbol{r})}{|(-\boldsymbol{r}\times\boldsymbol{v})\times(-\boldsymbol{r})|}\right)_z & \left(\dfrac{-\boldsymbol{r}\times\boldsymbol{v}}{|-\boldsymbol{r}\times\boldsymbol{v}|}\right)_z & \left(\dfrac{-\boldsymbol{r}}{|-\boldsymbol{r}|}\right)_z \end{bmatrix} \Delta \boldsymbol{v}^{LVLH} \tag{4}$$

where subscripts x, y and z denote the unit vector component of defined $\boldsymbol{r}$ in the M-MME2000 frame. Actually, $\Delta \boldsymbol{v}$ can be expressed as $\Delta \boldsymbol{v} = \Delta \boldsymbol{v}_{POD} + \Delta \boldsymbol{v}_{TST}$, where $\Delta \boldsymbol{v}_{POD}$ is the delta-V induced from the P-POD and $\Delta \boldsymbol{v}_{TST}$ is the delta-V induced from a thruster mounted on the CubeSat which should be regarded separately. However, the overall impulsive $\Delta \boldsymbol{v}$ is considered to simulate the CubeSat impact trajectory in this study as for a preliminary analysis. In Fig. 1, the defined geometry of the CubeSat impactor release conditions from the mother-ship is shown.

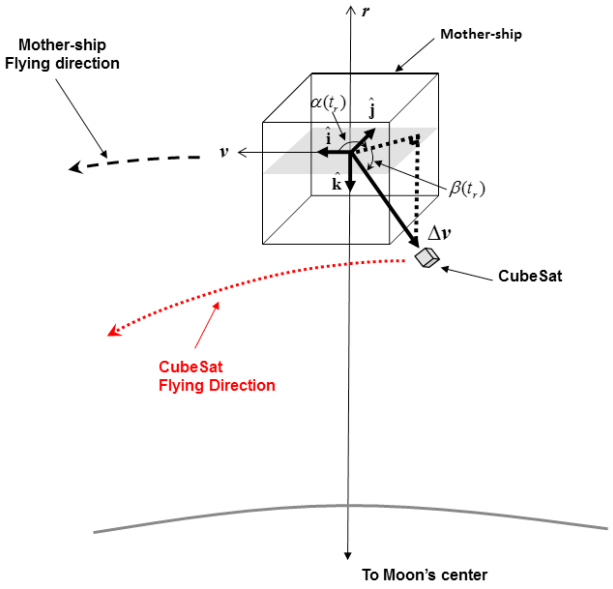

Fig. 1. Defined geometry of the CubeSat impactor release conditions from the mother-ship (not to scale).

After separation from the mother-ship, the deploy conditions that leads the CubeSat to impact the lunar surface can be selected using the method described by Brent (2002) which find the root of numerically integrated single nonlinear equation. During the root-finding process, the objective function, f_{obj}, is given as following:

$$f_{obj}(t_{app}) = |h_{Cube}| \tag{5}$$

By utilizing Eq. (5), the CubeSat impactor's closest approach time to the lunar surface, t_{app}, and the associated areodetic altitude, h_{Cube}, can be computed by determining whether the given objective function is increasing or decreasing within a user specified search interval of a lower and upper timeframe; t_{app}^{low} and t_{app}^{up}, respectively, as well as a user specified convergence criterion, ε_{root}. For this study, h_{Cube} is computed by applying a lunar flattening coefficient following a conversion of the CubeSat's states, which are originally expressed in the M-MME2000 frame, into the Moon Mean Equator and Prime Meridian (M-MMEPM) frame. If h_{Cube} is found to be greater than 0 km, then the CubeSat will not impact the lunar surface and will fly over with a determined h_{Cube} at t_{app}. If h_{Cube} is determined to be equal to 0 km, then there will be a lunar surface impact at t_{app}. t_{app} can thus be regarded as either the CubeSat impact time, t_{imp}, or the CubeSat Flight Time (CFT), t_{CFT}. In addition, at t_{imp} the areodetic longitude and latitude of the impact point $(\lambda(t_{imp}), \phi(t_{imp}))$ can be easily obtained from state components expressed in the M-MMEPM frame.

After the computed trajectory is found to be the impact cases, then, the CubeSat impact angle, $\theta(t_i)$, can be approximated as (Garrick-Bethell et al. 2013):

$$\theta(t_i) = \tan^{-1}\left(\frac{h(t_i)}{d(t_i)}\right) \tag{6}$$

where $h(t_i)$ is the mother-ship's areodetic altitude at every time instant during the impact phase, t_i, which ranges from $t_r \le t_i < t_{imp}$. $d(t_i)$ is the cross-range distance between the sub-ground point where the areodetic altitude is measured from $(\lambda(t_i), \phi(t_i))$ and the impact point $(\lambda(t_{imp}), \phi(t_{imp}))$. Thus, the cross-range distance can be regarded as a "travel

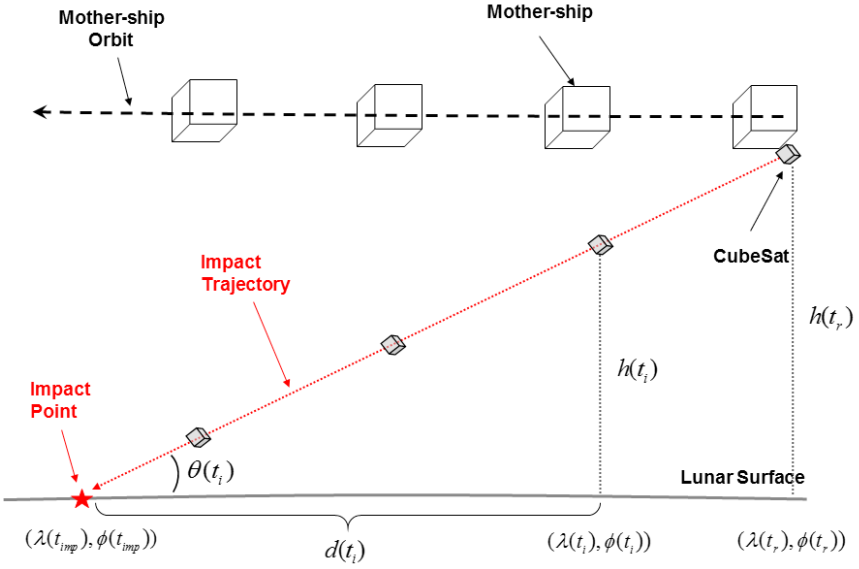

Fig. 2. Geometry of the defined CubeSat impact angle (not to scale).

distance" of the CubeSat measured on the lunar surface after separation. In Fig. 2, the defined CubeSat impact angle geometry is shown (Garrick-Bethell et al. 2013). The $d(t_i)$ between $(\lambda(t_i), \phi(t_i))$ and $(\lambda(t_{imp}), \phi(t_{imp}))$ is computed by the method described by Sodano (1965) and is given as follows:

$$\begin{aligned} d(t_i) = r_{pol}\Bigg(&\left[(1+f+f^2)\delta\right] \\ &+ r_{Moon}\left[[(f+f^2)\sin\delta - \left(\frac{f^2}{2}\right)\delta^2\csc\delta]\right] \\ &+ \xi\left[-\left(\frac{f+f^2}{2}\right)\delta - \left(\frac{f+f^2}{2}\right)\sin\delta\cos\delta + \left(\frac{f^2}{2}\right)\delta^2\cot\delta\right] \\ &+ r_{Moon}^2\left[-\left(\frac{f^2}{2}\right)\sin\delta\cos\delta\right] \\ &+ \xi^2\left[\left(\frac{f^2}{16}\right)\delta + \left(\frac{f^2}{16}\right)\sin\delta\cos\delta - \left(\frac{f^2}{2}\right)\delta^2\cot\delta - \left(\frac{f^2}{8}\right)\sin\delta\cos^3\delta\right] \\ &+ r_{Moon}\xi\left[\left(\frac{f^2}{2}\right)\delta^2\csc\delta + \left(\frac{f^2}{2}\right)\sin\delta\cos^2\delta\right]\Bigg) \end{aligned} \tag{7}$$

In Eq. (7), r_{pol} and r_{Moon} are the Moon's mean polar radius and mean equatorial radius, respectively. f is the Moon's flattening coefficient where $f = 1 - (r_{pol}/r_{Moon}) \approx 0.0012$. δ and ξ are parameters defined as follows:

$$\delta = \tan^{-1}\left(\frac{(\sin\varepsilon_1\sin\varepsilon_2) + (\cos\varepsilon_1\cos\varepsilon_2)\cos\lambda}{\sqrt{(\sin\lambda\cos\varepsilon_2)^2 + \left[\sin(\varphi_2 - \varphi_1) + 2\cos\varepsilon_2\sin\varepsilon_1\sin^2(\lambda/2)\right]^2}}\right) \tag{8}$$

$$\xi = 1 - \left(\frac{(\cos\varepsilon_1\cos\varepsilon_2)\sin\lambda}{\sin\delta}\right)^2 \tag{9}$$

where

$$\lambda = \lambda(t_{imp}) - \lambda(t_i) \tag{10}$$

$$\varepsilon_1 = \tan^{-1}\left(\frac{r_{pol}\sin\phi(t_i)}{r_{Moon}\cos\phi(t_i)}\right) \tag{11}$$

$$\varepsilon_2 = \tan^{-1}\left(\frac{r_{pol}\sin\phi(t_{imp})}{r_{Moon}\cos\phi(t_{imp})}\right) \tag{12}$$

$$\begin{aligned} \varphi_2 - \varphi_1 &= \left(\phi(t_{imp}) - \phi(t_i)\right) \\ &+ 2\left[\sin\left(\phi(t_{imp}) - \phi(t_i)\right)\right]\left[(\eta + \eta^2 + \eta^3)r_{Moon} - (\eta - \eta^2 + \eta^3)r_{pol}\right] \end{aligned} \tag{13}$$

$$\eta = \left(\frac{r_{Moon} - r_{pol}}{r_{Moon} + r_{pol}}\right) \tag{14}$$

For the CubeSat onboard thruster, the required burn duration during the divert phase, t_{burn}, can be approximated by:

$$t_{burn} = \frac{(m_{fuel})g_0 I_{sp}}{T} \tag{15}$$

where g_0 is the gravitational acceleration, I_{sp} is the specific impulse of the thruster, T is the thrust magnitude and m_{fuel} is the required fuel mass. m_{fuel} can be derived as:

$$m_{fuel} = m_0\left[1 - \exp\left(-\frac{\Delta v}{g_0 I_{sp}}\right)\right] \tag{16}$$

The approximated mass after burnout, m_f, can then be easily obtained with $m_f = m_0 - m_{fuel}$, where m_0 is the CubeSat's initial mass.

3. SIMULATION SETUP

To simplify the given problem so as to focus on early design phase analysis, several assumptions are made during the simulations. As previously discussed, two-body equations of motion are used to simulate both the mother-ship and the CubeSat impactor. Divert delta-V is assumed to be an impulsive burn for the CubeSat impactor separation. For numerical integration, a Runge-Kutta-Fehlberg 7-8th order variable step size integrator is used with a truncation error tolerance of $\varepsilon = 1 \times 10^{-12}$. To convert the coordinate system between the M-MME2000 and M-MMEPM frames, the lunar orientation specified by JPL DE405 is used (Standish 1998). It is assumed that the CubeSat impactor is deployed at the moment when the mother-ship is flying over the northern polar region of the Moon, and is assumed to have a circular, 90 deg inclined polar orbit. Four different orbital altitudes are considered; 50, 100, 150 and 200 km. Thus, the initial orbital components for the mother-ship expressed in the M-MME2000 frame are given as: zero eccentricity, 90 deg inclination, 0 deg right ascension of the ascending node, 90 deg argument of latitude, and semi-major axes of about 1,788.2, 1,838.2, 1,888.2 and 1,938.2 km for its different orbital altitudes, respectively. The initial epoch of the CubeSat impactor release is assumed to be July 1st 2017, corresponding to Korea's first experimental lunar orbiter mission, which is currently planned to be launched in 2017. For release directions, the out-of-plane release direction is increased from 90 deg to 180 deg at 0.5 deg increments. This indicates that the CubeSat impactor will always be deployed in the opposite direction of the mother-ship flight direction so as to not to interfere with the mother-ship's original flight path. The in-plane release are constrained to 0 deg at all times so as to not cause plane changes during the impact phase. The divert delta-V magnitudes are increased from 0 m/s to 90 m/s at 0.5 m/s increments. For the impact conditions derivation, the convergence criterion is given as $\varepsilon_{root} = 1 \times 10^{-12}$. During the analysis, out of the numerous impact trajectories that

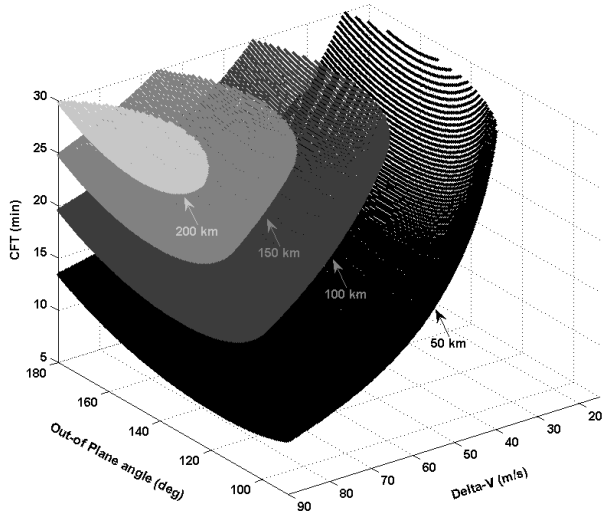

Fig. 3. CubeSat flight time characteristics as a function of divert delta-V and out-of-plane direction release angle at four different release altitudes (50, 100, 150 and 200 km).

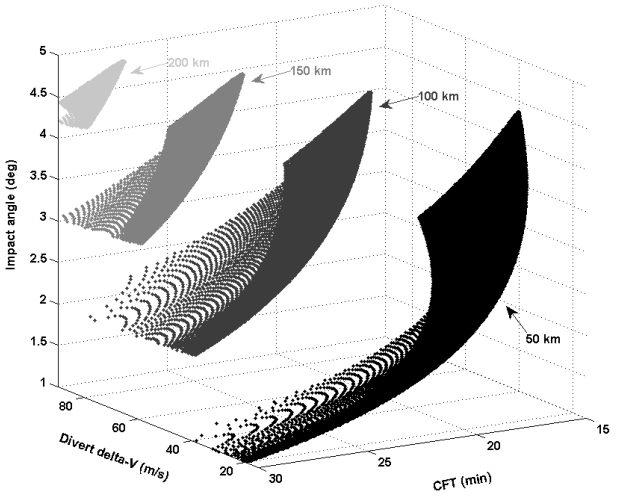

Fig. 4. CubeSat impact angle characteristics as a function of divert delta-V and the CubeSat flight time at four different release altitudes (50, 100, 150 and 200 km).

are discovered, trajectories that have a CFT of more than 30 min are not considered as the current CubeSat impactor mission will only be operated with a charged battery during the impact phase, which is expected to support maximum of about 30 min. Impact trajectories showing impact angles greater than 10 deg are also not considered, as they would violate the impact angle requirement of the CubeSat impactor given to achieve the science goals (Garrick-Bethell et al. 2013). The initial overall mass of the CubeSat impactor is assumed to be 5 kg, including payload, fuel and bus structure masses

4. RESULTS ANALYSIS

4.1 Impact Trajectory Characteristics Deployed from Different Altitudes

In this sub-section, the characteristics of CubeSat impact trajectories as a function of its release conditions (divert delta-V and out-of-plane direction release angle) for four different altitudes (50, 100, 150 and 200 km) are analyzed. Critical design parameters that are directly related to the success of the mission are also analyzed including the CFT, impact velocity, and impact angles. In Fig. 3, the characteristics of CFTs as a function of deploy delta-V magnitude and out-of-plane deploy direction angle are shown at four different release altitudes. Note that CFT is numerically determined with the conditions shown in Eq. (5), and the deploy delta-V magnitude for both out-of and in-plane deploy direction angles are given arbitrary values as discussed in the previous section. Impact velocity is directly derived by numerically integrating the CubeSat impact trajectory. Characteristics of the CubeSat impact angle (derived using Eq. (6)) as a function of divert delta-V magnitude and CFT are also shown in Fig. 4. In this simulation, cross-range distance (Eq. (7)) is computed at the sub-satellite point where the CubeSat is released ($\lambda(t_r)$, $\phi(t_r)$) in order to compute the impact angle, and is taken as a reference values. However, note that the resulting impact angle could slightly change at any moment during the impact phase as it is dependent on the point from where the cross-ranges are measured.

From Fig. 3, it can be concluded that the higher the release altitude, the more deploy delta-V is required to release the CubeSat in order to impact the lunar surface. As the release altitude increases, acceptable out-of-plane deployment ranges become narrower. The resultant CFT also exhibit higher values at these narrower boundaries. These results indicate that release conditions of smaller values are possible in order to meet the science objectives if the CubeSat is released at higher altitudes. For example, it is certain that releasing the CubeSat at a 50 km altitude has more opportunities for impact than when released from a 200 km altitude as the 50 km case has wider ranges of divert delta-Vs, out-of-plane angle release directions, and CFTs. Less divert delta-Vs and wider ranges of CTF will certainly ease the design process of the onboard propulsion system as they are directly related to the size of the propulsion system. For impact angle characteristics, regardless of release altitude, the mission requirements were satisfactorily achieved as they all remained less than 4.81 degs. Taking the impact angle as the major design parameter, it seems

that a CubeSat release at a 200 km altitude would be the most effective choice as this angle shows greater impact angle ranges (4.20 ~ 4.81 degs) as compared with releases from other altitudes (1.00 ~ 3.47 degs for 50 km release case, for example). In addition, a 200 km release altitude can partially avoid the uncertainties inherent lunar surface heights. However, as seen in Fig. 3, it should be noted that releasing the CubeSat from a 200 km altitude requires a higher deploy delta-V magnitude (76.5 ~ 88.0 m/s) than at other heights. These values in these ranges are quite large to be supported by the onboard thruster of the CubeSat for given CFTs. Careful trade-off studies should therefore be made in future analyses to select the most appropriate candidate for the onboard thrusters. In Table 1, detailed characteristics of the obtained CubeSat impact trajectories are summarized including minimum and maximum values of deploy delta-Vs, out-of-plane angle, CFT, impact velocity and impact angles. From Table 1, variation tendencies in CubeSat impact trajectories at different release altitudes can be easily observed.

4.2 Divert Burn Characteristics for Different onboard Thrusters

As the capabilities of the CubeSat missions are increasing, such as orbit raising, orbital plane change, formation flying, fine attitude control, proximity operation, and de-orbit, onboard propulsion capabilities for the CubeSat are becoming a more crucial factor for the success of the mission. Indeed, there exist various options that can be used for the onboard CubeSat thrusters, including monopropellants, bipropellants, solid propellants with cold gas for chemical thrusters, vacuum arc, micro scale retro jets, micro pulsed plasma, and micro colloid for electric thrusters (Storck et al. 2006). Aside from these thrusters, readers can find numerous propulsion systems that are possible for CubeSats in Mueller et al. (2010). Based on the divert delta-V characteristics previously derived, this sub-section analyzes divert burn characteristics such as required burn time and fuel mass using four arbitrarily selected CubeSat onboard thrusters. Four different miniaturized onboard thrusters commercially developed for CubeSat applications are considered and are shown in Table 2. Selection of onboard thruster is made by trial and error during the simulation to not only to provide a wide range of thrust magnitude but also to obtain meaningful results under the divert delta-Vs obtained previously. For the following discussions, fuel mass and burn time fraction are computed through $(m_{fuel}/m_0)\times 100$ and $(t_{burn}/t_{CFT})\times 100$, respectively. During the estimation of m_{fuel} (shown in Eq.(16)), 2.0 m/s of delta-V (currently available delta-V magnitude with P-POD separation mechanism using P-POD Mk. III (Lan et al. 2007) is subtracted from the values of the obtained delta-V, Δv, as the current study only considers the overall divert delta-Vs in order to hit the lunar surface.

In Fig. 5, burn time fraction characteristics as a function of divert delta-V and out-of-plane release angle for four different deployment altitudes are shown for four different onboard thruster model. Figs. 5(a)-5(d) correspond to the onboard thruster models A, B, C, and D, respectively, listed in Table 2. With thruster models A and B, it is possible to impact the lunar surface within a required CTF at each altitude (50, 100, 150 and 200 km). Deployed and burn time fraction is found to be about 0.12~1.48% for thruster model A and 0.17~2.18% for the thruster model B. This indicates that an engine burn duration of only 2% of the

Table 1. Detailed design parameters for the obtained CubeSat impact trajectories at different orbital release altitudes.

Release Altitude (km)	Delta-V (m/s)		Out-of-plane angle (deg)		Impact Velocity (km/s)		CFT (min)		Impact Angle (deg)	
	Min.	Max.	Min.	Max.	Min.	Max.	Min.	Max.	Min.	Max.
50	17.50	88.00	90.00	180.00	1.61	1.71	8.88	30.00	1.00	3.47
100	37.00	88.00	91.50	180.00	1.64	1.72	15.66	30.00	1.98	3.98
150	56.50	88.00	105.00	180.00	1.67	1.73	21.50	30.00	3.03	4.44
200	76.50	80.00	123.50	180.00	1.68	1.74	26.94	30.00	4.20	4.81

Table 2. Characteristics of four different miniaturized onboard thrusters used for this simulation.

	Manufacturer	Model	Thrust mag. (N)	Isp (sec)
Model A (Mueller et al. 2010)	Moog	50-820	52	65
Model B (Zondervan et al. 2014)	Aerospace Corporation	ISP 30	37	187
Model C (BUSEK, 2014)	BUSEK	Green Monopropellant Thruster	0.5	250
Model D (Mueller et al. 2010)	Moog	58E151	0.12	65

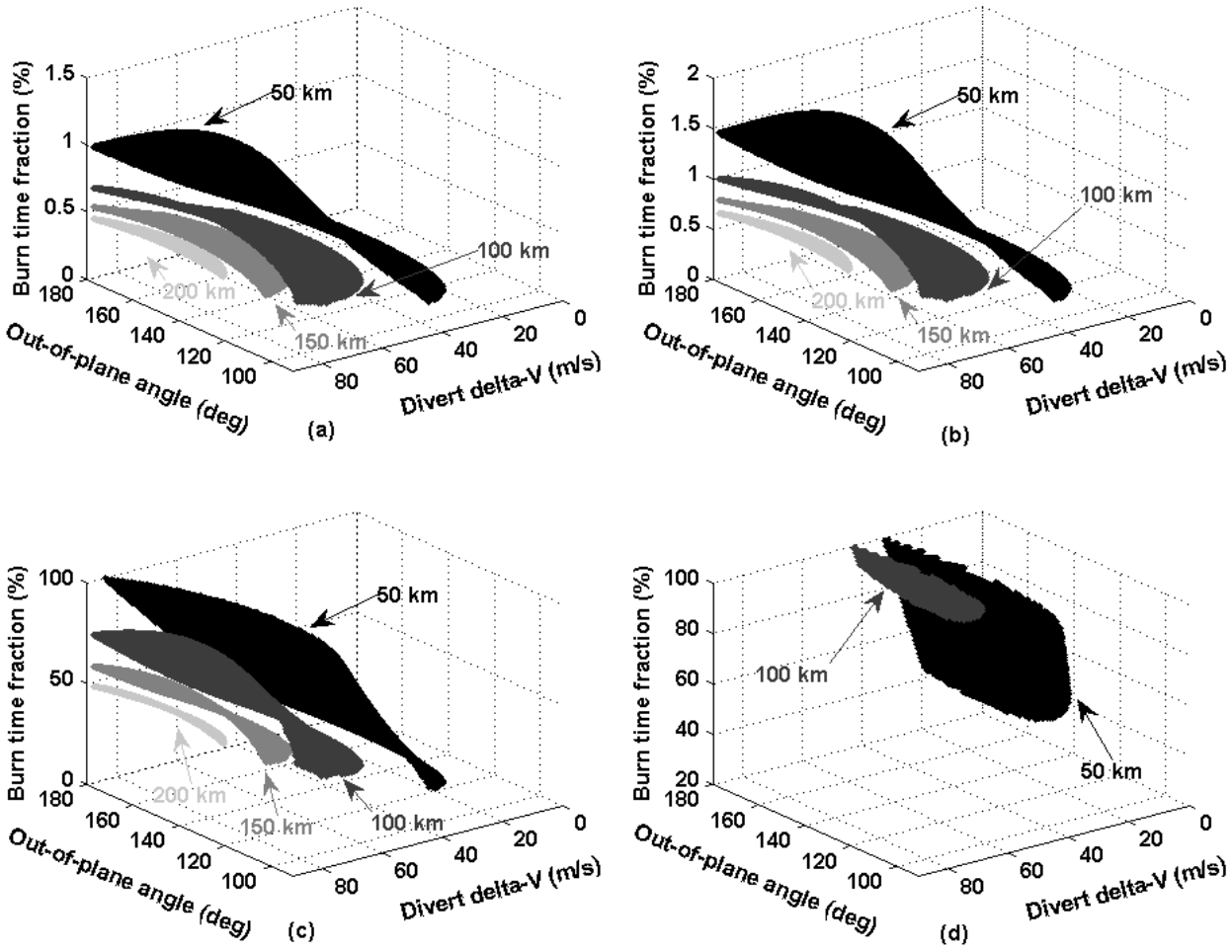

Fig. 5. Burn time fraction characteristics four different deployment altitudes for four different onboard thruster models; (a) thruster model A, (b) model B, (c) model C, and (d) model D.

entire CFT is necessary during the CubeSat impact phase if a thruster is used that has similar performance to those of the selected thrusters. However, with thruster model C, burn time fraction reaches up to about 99.99% for the 50 km altitude deployment case as shown in Fig. 5(c). This means that the onboard thruster would have to be turned on for the entire duration of the lunar impact phase. Running the thruster during the entire impact phase could lead to serious difficulties in attitude control strategy of the CubeSat and could also affect the qualities of science data gathered. Similarly, burn time fraction with thruster model D also reaches 100%. It is found that only the 50 and 100 km altitude deployed cases are partially available to impact the lunar surface. Therefore, CubeSats deployed from 150 and 200 km altitudes with thruster model D are not able to impact the lunar surface as every required delta-V cannot be supported within the required CFTs. As clearly shown in Fig. 5(d), very limited ranges of divert delta-V can be covered with thruster model D. From the burn time fraction point of view, it seems that an onboard thruster's performance equivalent to those of model A, B and C would be acceptable for future lunar CubeSat impactor missions. However, achieving the target impact point with models A and B would be more critical than with the model C. This is because fine targeting of the impact point through higher thrust levels would very difficult to achieve requiring complex thruster on-off strategies resulting in an increase in complexity of the CubeSat operation concept. Therefore, it seems that having an onboard thruster whose performance is equivalent to or slightly better than that of model C will more be preferable as every CubeSat deployment altitude (except minor part of 50 km release case) can be covered with reasonable burn time fractions, roughly about 50%, with thruster model C. The authors believe that securing an appropriate free flight path during the impact phase will be critical for the success of the mission as a constant thruster burn during most of the impact phase could lead to not only serious difficulties in attitude control but also

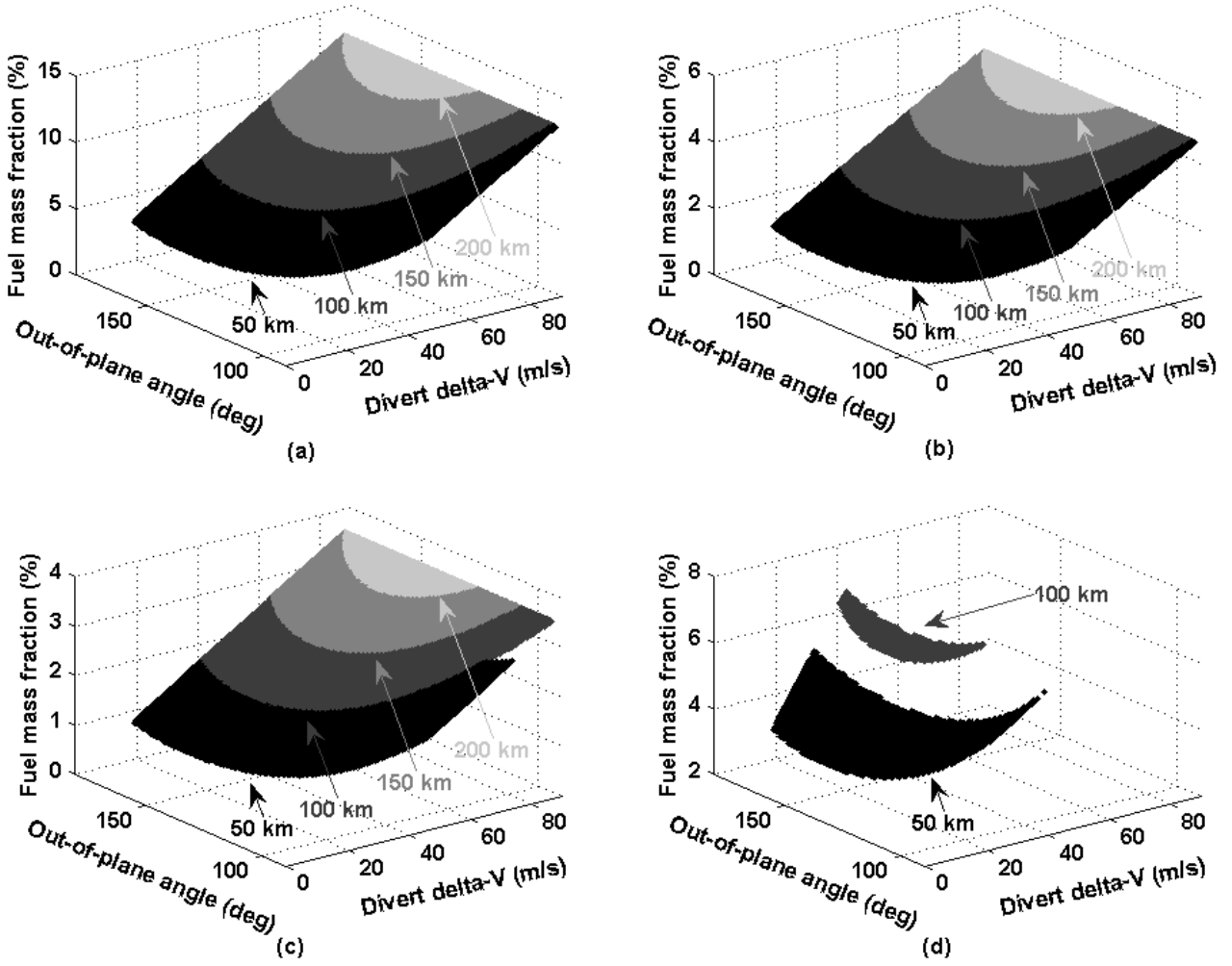

Fig. 6. Fuel mass fraction characteristics for four different deploy altitudes for four different onboard thruster models; (a) thruster model A, (b) model B, (c) model C, and (d) model D.

could affect the qualities of science data gathered due to the disturbances. Similarly for those in Fig. 5, fuel mass fraction characteristics are analyzed and depicted in Fig. 6. Figs. 6(a)-6(d) correspond to thruster models A, B, C, and D, respectively. Regardless of deployment altitude and onboard thruster, the fuel mass fractions remained within the ranges of 2.71~12.89% with thruster model A, 0.95~4.69% with model B, 0.71~3.52% with model C, and 2.71~6.67% with model D. The maximum obtained fuel mass fraction is about 12.89% when deployed from a 200 km altitude with thruster model A, which is only about 0.64 kg out of the CubeSat's total 5 kg mass. With thruster model C, it is found that only about 0.17 kg of fuel is necessary to accomplish the impact mission with a suitable burn time fraction. Detailed mission parameters derived for each onboard thruster is summarized in Table 3. From the previous burn time and fuel mass fraction analyses, it can be concluded that during the design stage of the onboard thrusters for a CubeSat lunar impact mission, thrust burn time should be more critically considered as a design parameter than the required fuel mass for the impact phase of the mission.

An example of an impact trajectory is shown in Fig. 7. In this example, the CubeSat is assumed to be released at an altitude of 100 km with an 180 deg out-of-plane angle and 60 m/s divert delta-V. Thruster model C is assumed to be installed. In the figure, the trajectories are shown with the normalized distance unit, Lunar Unit (LU), where 1 LU is approximately 1,738.2 km. For the actual flight, some time gaps may be required between the moment of the CubeSat separation and the ignition of onboard thruster for mission safety. For this study, however, the onboard thruster is assumed to be turned-on just after the CubeSat separation. For this example, it is found that about 24.50 min of CFT is required to impact the lunar surface with an impact velocity and angle of about 1.67 km/s and 2.57 deg, respectively. With the model C onboard thruster, about 9.55 min of burn

Table 3. Detailed design parameters for selected onboard thrusters for different orbital deployment altitudes. Assumed overall CubeSat mass to be 5 kg.

Thruster Model	Release Altitude (km)	Fuel mass fraction (%)		Required fuel mass (kg)		Burn time Fraction (%)		Burn time (min)	
		Min.	Max.	Min.	Max.	Min.	Max.	Min.	Max.
A	50	2.71	12.89	0.14	0.64	0.09	1.48	0.03	0.13
	100	5.64	12.89	0.28	0.64	0.19	0.84	0.06	0.13
	150	8.48	12.89	0.42	0.64	0.29	0.61	0.08	0.13
	200	11.31	12.89	0.57	0.64	0.39	0.49	0.12	0.13
B	50	0.95	4.69	0.05	0.23	0.13	2.18	0.04	0.19
	100	2.00	4.69	0.10	0.23	0.28	1.24	0.08	0.19
	150	3.03	4.69	0.15	0.23	0.42	0.90	0.13	0.19
	200	4.09	4.69	0.20	0.23	0.56	0.72	0.17	0.19
C	50	0.71	3.37	0.04	0.18	9.70	99.98	2.91	13.76
	100	1.50	3.53	0.07	0.18	20.41	92.01	6.12	14.41
	150	0.11	0.18	0.11	0.18	31.03	67.01	9.31	14.41
	200	3.07	3.52	0.15	0.18	41.83	53.47	12.55	14.41
D	50	2.71	6.23	0.14	0.32	39.99	99.99	11.99	27.58
	100	5.64	6.67	0.28	0.33	83.24	99.99	24.96	29.52
	150	N/A	N/A	N/A	N/A	N/A	N/A	N/A	N/A
	200	N/A	N/A	N/A	N/A	N/A	N/A	N/A	N/A

duration out of 24.50 min of CFT is necessary to satisfy the delta-V required for successful lunar surface impact, which is about 38.98% of burn time. As shown in Fig. 7, for the remaining 41.02% of the impact phase, the CubeSat will freely fly towards the lunar surface with the thruster off. During this phase, science data gathering could be done with less disturbances that can affect the quality of the data. Additionally, about 0.12 kg of fuel is required with this thruster model. From the assumed overall CubeSat mass of 5 kg, the final mass of the CubeSat after the burn will be about 4.88 kg, resulting in a fuel mass fraction of about 2.34%.

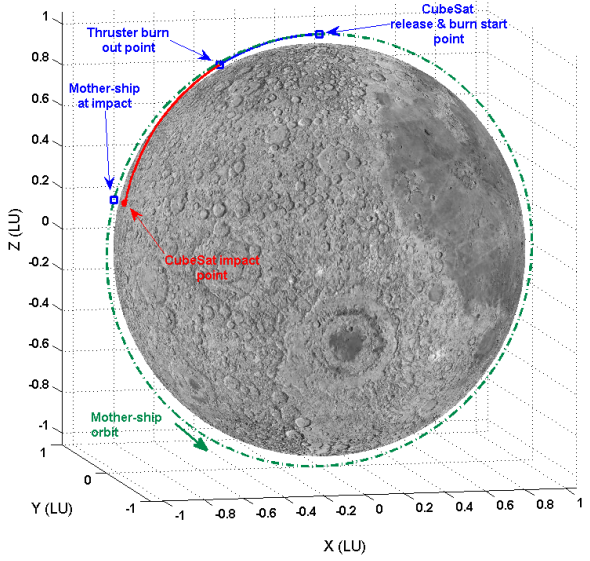

Fig. 7. Example of impact trajectory of a CubeSat released from a 100 km altitude with thruster model C.

5. CONCLUSIONS

As a part of early system design activities for a lunar CubeSat impactor mission, this study analyzes characteristics of delta-V requirements in order to deploy an impactor from a mother-ship orbiting the Moon with a circular orbit, 90 deg inclination, and having different orbital altitudes (50, 100, 150, 200 km). Along with delta-V requirements, deploy directions, CubeSat flight time, impact velocity, and associated impact angles are also analyzed. Required onboard thruster burn time and required fuel mass are analyzed as well by adapting four different miniaturized commercial onboard thrusters currently developed for CubeSat applications. As a result, it is discovered that if the CubeSat is released at higher altitudes, lesser release conditions are achievable to meet the mission objectives. This is due to the fact that deploying at higher altitudes require more deploy delta-V, limited ranges of out-of-plane deploy angle, and longer CubeSat flight time. However, high altitude deployment of the CubeSat can partially avoid the uncertainties bared in lunar surface heights as a result of the higher impact angle as compared with the lower altitude deployment cases. From deployment burn characteristics analysis results, it is estimated that an onboard thruster having a performance equivalent to about 0.5 N of thrust and with an Isp of 250 sec (slightly better will more be preferable) would be acceptable for the future lunar CubeSat impactor mission having 5 kg of overall mass. For this case, a maximum of about 0.18 kg of fuel is required to impact the CubeSat regardless of deployment altitude. With an onboard thruster of this performance, burn time fraction was found to be roughly about 50% of the 30 min total CubeSat flight time. This indicates that the CubeSat can freely fly toward the lunar

surface with the thruster turned off for almost half of its entire impact phase. In addition, it is concluded that thrust burn time should be the more closely considered design parameter than the required fuel mass when determining the onboard propulsion system requirements for this kind of impactor mission. Results provided in this study will be helpful in further defining detailed system and design activities for future lunar missions with a CubeSat-based payload.

ACKNOWLEDGEMENTS

This work was supported by the Korea Aerospace Research Institute's (KARI) research project FR15530. Also, partially supported by the BK21 Plus and NRF-2014M1A3A3A02034761 Program through the National Research Foundation (NRF), funded by the Ministry of Education and the Ministry of Science, ICT and Future Planning of South Korea.

REFERENCES

Blaney DL, Staehle RL, Betts B, Friedman L, Hemmati H, et al., Interplanetary CubeSats: Small, low cost missions beyond low Earth Orbit, Proceedings of the 43rd Lunar and Planetary Science Conference, Woodlands, Texas, 19-23 Mar 2012.

Brent, RP, Algorithms for minimization without derivatives. (Dover publication, Mineola, 2002), 18-79.

BUSEK, Green Monopropellant Thrusters [Internet], cited 2014 Dec. 12, available from: http://www.busek.com/technologies_greenmonoprop.htm

Curtis HD, Orbital Mechanics for Engineering Students, 2nd ed. (Elsevier, Oxford, 2009), 61-69.

Eom WS, Kim YK, Lee JH, Choi GH, Sim ES, Study on a suspension of a planetary exploration rover to improve driving performance during overcoming obstacles, J. Astron. Space Sci. 29, 381-387 (2012).

Garrick-Bethell I, Lin RP, Sanchezd H, Jaroux BA, Bester M, et al., Lunar magnetic field measurements with a cubesat, in proceedings of the SPIE Defense, Security, and Sensing, Baltimore, Maryland, 21 May 2013.

JPL (Jet Propulsion Laboratory), JPL Selects Europa CubeSat Proposals for Study, [Internet], cited 2014 Oct. 23, available from: http://www.jpl.nasa.gov/news/news.php?feature=4330

Kim YK, Kim HD, Lee JH, Sim ES, Jeon SW, Conceptual design of rover's mobility system for ground-based model, J. Astron. Space Sci. 26, 677-692 (2009).

Klesh AT, Castillo-Rogez JC, Applications of NanoSats to Planetary Exploration, Proceedings of the AIAA SPACE 2012 Conference & Exposition, Pasadena, California, 11-13 Sep 2012.

Komarek T, Bailey Z, Schone H, Jedrey T, Chandler A, Novel Ideas for Exploring Mars with CubeSats: Challenges and Possibilities, Proceedings of the 10th IAA Low-Cost Planetary Missions Conferences, Pasadena, California, 18-20 June 2013.

Lan W, Munakata R, Nugent LR, Pignatelli D, Poly Picosatellite Orbital Deployer Mk. III Rev. E User Guide [CP-PPODUG-1.0-1] (California Polytechnic State University, San Luis, 2007), 1-5.

Lee HJ, Lee JK, Baek SM, Kim KH, Jin H, et al., A CubeSat Mission for Korean Lunar Exploration, Proceedings of the 45th Lunar and Planetary Science Conference, Woodlands, Texas, 17-21 Mar 2014.

Mueller J, Hofer R, Ziemer J, Survey of propulsion technologies applicable to cubesats, Proceedings of 57th Joint Army-Navy-NASA-Air Force (JANNAF) Propulsion meeting, Colorado Springs, Colorado, 3 May 2010.

Sodano EM, General non-iterative solutions of the inverse and direct geodetic problems, Bulletion Géodésique 75, 69-89 (1965).

Song YJ, Woo J, Park SY, Choi KH, Sim ES, The earth moon transfer trajectory design and analysis using intermediate loop orbits, J. Astron. Space Sci. 26, 171-186 (2009).

Song YJ, Park SY, Kim HD, Lee JH, Sim ES, Analysis of delta-V losses during lunar capture sequence using finite thrust, J. Astron. Space Sci. 28, 203-216 (2011).

Song YJ, Ahn SI, Choi SJ, Sim ES, Ground contact analysis for korea's fictitious lunar orbiter mission, J. Astron. Space Sci. 30, 255-267 (2013).

Song YJ, Choi SJ, Ahn SI, Sim ES, Analysis on tracking schedule and measurements characteristics for the spacecraft on the phase of lunar transfer and capture" J. Astron. Space Sci. 31, 51-61 (2014).

Song YJ, Jin H, Garick-Bethell I, Lunar CubeSat Impact Trajectory Characteristics as a Function of Its Release Conditions, Math. Probl. Eng. 2015, Article ID 681901 (2015). http://dx.doi.org/10.1155/2015/681901

Staehle RL, Blaney B, Hemmati H, Jones D, Klesh AT et al., Interplanetary CubeSats: Opening the Solar System to a Broad Community at Lower Cost, J. Small Satell. 2, 161-186 (2013).

Standish EM, JPL planetary and lunar ephemerides, DE405/LE405 (Jet Propulsion Laboratory, Los Angeles, 1998), 1-6.

Storck W, Billet O, Jambusaria M, Sadhwani A, Jammes P, et al. A Survey of Micro-propulsion for Small Satellites, Proceedings of the 20th Annual Small Satellite Conference, Ogden, Utah, 14-17 Aug 2006.

Swartwout M, The First One Hundred CubeSats: A Statistical Look, J. Small Satell. 2, 213-233 (2013).

Vallado DA, Fundamentals of astrodynamics and applications, 4th ed. (Kluwer Academic Publishers, Boston, 2013), 151-169.

Woo J, Song YJ, Park SY, Kim HD, Sim ES, An earth-moon transfer trajectory design and analysis considering spacecraft's visibility from daejeon ground station at TLI and LOI maneuvers, J. Astron. Space Sci. 27, 195-204 (2010).

Zondervan K, Fuller J, Rowen D, Hardy B, Kobel C, et al., CubeSat Solid Rocket Motor Propulsion Systems providing Delta-Vs greater than 500 m/s, Proceedings of the 28th Annual Small Satellite Conference, Logan, Utah, 2-7 Aug 2014.